

Variational method for the $Z(2)$ gauge model

D. Boyanovsky, R. Deza, and L. Masperi

Centro Atómico Bariloche, Comisión Nacional de Energía Atómica and Instituto Balseiro, Universidad Nacional de Cuyo 8400 S. C. de Bariloche, R. N. -Argentina

(Received 10 September 1979; revised manuscript received 7 July 1980)

A variational method similar to the one used for the Ising model is applied to the Hamiltonian $Z(2)$ lattice gauge theory in three dimensions. It is shown that the proposal of a gauge-invariant ground state leads to a transition in the Wilson loop integral from the area to the perimeter behavior for a value of the coupling constant close to the symmetry point predicted by self-duality. The discontinuity which appears in the variational parameter gives strong evidence in favor of the first-order nature of the transition in contrast to what occurs for the two-dimensional model.

I. INTRODUCTION

The $Z(N)$ gauge models, the center of the $SU(N)$ theories, seem to be crucial for the quark-confinement problem.¹ They are also of great interest for being the simplest gauge theories obtained from the well-known Ising model,² and are connected with spin-glass models³ and the two-dimensional melting theory.⁴

The Ising models show second-order phase transitions characterized by the appearance of a nonvanishing local order parameter, the magnetization. The properties of both phases can be described in the Hamiltonian formalism by perturbative calculations starting from the extreme ground states.⁵ The actual values of the critical coupling constant may be obtained using the renormalization group through different versions of block-spin techniques.⁶ The general features of the phase transition, though with less accurate values of the critical parameters, can also be obtained with simpler variational methods of the mean-field type.⁷

Going to the lattice gauge theories, mean-field arguments suggest the existence of first-order transitions⁸ based on the abrupt appearance of a local order parameter. However, the proof that the ground state of a gauge theory must be gauge invariant⁹ forbids the existence of nonvanishing expectation values of gauge-dependent operators. It is therefore necessary to consider a nonlocal gauge-invariant order parameter, i.e., the Wilson loop integral.¹⁰ Again, perturbative calculations show the existence of two phases characterized by the loop-area or loop-perimeter behavior.⁵

The requirement of gauge invariance of the ground state considerably complicates the block-spin calculations. Using these techniques the Hamiltonian $Z(2)$ gauge model in two spatial dimensions has been analyzed¹¹ showing a second-order phase transition, as expected since this model is dual to the Ising model with transverse field

in two dimensions.

Regarding the $Z(2)$ model in three spatial dimensions, Monte Carlo calculations¹² have indicated the appearance of features characteristic of first-order transitions, which disappear in the two-dimensional model. In contrast a renormalization-group method¹³ for the Hamiltonian model shows for the three-dimensional case a second-order transition too. The same result emerges from the renormalization-group treatment in the Lagrangian formalism.¹⁴

The purpose of this work is to analyze the Hamiltonian $Z(2)$ gauge model in three spatial dimensions using the simplest technique to demonstrate the features of the phase transition, i.e., a variational method of the mean-field type. Though one cannot expect a very accurate description of the critical phenomenon, one may hope in this way to distinguish between a first- and a second-order phase transition.

In Sec. II we recall the properties of this variational method applied to the Hamiltonian Ising model with transverse field in one spatial dimension to show its usefulness in understanding the phase transition and its limitations regarding the critical coupling constant compared to the exact value.

In Sec. III we apply the variational method to the $Z(2)$ gauge model with the requirement of gauge invariance of the ground state. Introducing the Wilson loop integral as a criterion for the phase characterization it turns out that, exploiting the self-dual property of $Z(2)$ in three spatial dimensions, this nonlocal parameter changes from an $\exp(-\text{loop area})$ to an $\exp(-\text{loop perimeter})$ behavior when the coupling constant increases.

Because of numerical complications, it is not possible to consider exactly a system with a too large number of sites. Therefore, in Sec. IV the variational method is expressed in the form of an analogous classical three-dimensional Ising model which allows the use of high- and low-

temperature expansions extrapolated by means of Padé approximants. It is possible to appreciate the first-order nature of the transition in the three-dimensional case through a discontinuity of the variational parameter which appears when the coupling constant crosses a value in quite good agreement with that expected by self-duality. When the same method is applied to the two-dimensional model one may still define a phase transition but without discontinuity of the variational parameter consistently with its second-order nature.¹⁵

A few concluding remarks are contained in Sec. V.

II. HAMILTONIAN ISING MODEL IN ONE DIMENSION

We start analyzing this well-known case with the variational method. The Hamiltonian in terms of Pauli matrices

$$H = - \sum_n \sigma_1(n) - \lambda \sum_n \sigma_3(n) \sigma_3(n+1) \quad (1)$$

is self-dual since, defining according to Fig. 1

$$\tilde{\sigma}_1(\tilde{n}) = \sigma_3(n) \sigma_3(n+1), \quad \tilde{\sigma}_3(\tilde{n}) = \sum_{m \leq n} \sigma_1(m), \quad (2)$$

we obtain

$$\begin{aligned} \tilde{H} &= H/\lambda \\ &= - \sum_{\tilde{n}} \tilde{\sigma}_1(\tilde{n}) - \lambda^{-1} \sum_{\tilde{n}} \tilde{\sigma}_3(\tilde{n}) \tilde{\sigma}_3(\tilde{n}+1), \end{aligned} \quad (3)$$

showing that the phase transition must occur at the symmetry point $\lambda = 1$.

If we make the mean-field assumption that all spins behave in the same way and write the ground state as⁷

$$|\theta\rangle = \sum_{\text{sites}} \begin{pmatrix} \cos \frac{1}{2} \theta \\ \sin \frac{1}{2} \theta \end{pmatrix}_n, \quad (4)$$

the energy

$$E(\theta) = \langle \theta | H | \theta \rangle = -N_s (\sin \theta + \lambda \cos^2 \theta) \quad (5)$$

has two minima: (i) $\cos \theta = 0$, $E_1 = -N_s$; (ii) $\sin \theta = 1/2\lambda$, $E_2 = -N_s(\lambda + 1/4\lambda)$, where N_s is the number of sites.

For $\lambda < \frac{1}{2}$ the second solution is impossible and the ground state is given by Fig. 2(a). For $\lambda > \frac{1}{2}$ the second solution has lower energy and corresponds to the doubly degenerate ground state of

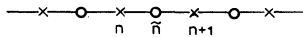


FIG. 1. Using one-dimensional lattice. Crosses denote direct sites and open circles denote dual sites.

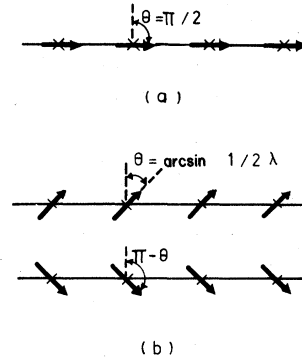


FIG. 2. Using variational ground states. (a) Nondegenerate state for $\lambda < \frac{1}{2}$; (b) doubly degenerate state for $\lambda > \frac{1}{2}$.

Fig. 2(b).

The order parameter is

$$\langle \theta | \sigma_3(n) | \theta \rangle = \begin{cases} 0, & \text{for } \lambda < \frac{1}{2} \\ \cos \theta, & \text{for } \lambda > \frac{1}{2} \end{cases}$$

where the upper degenerate state has been taken for $\lambda > \frac{1}{2}$. The critical point occurs at $\lambda = \frac{1}{2}$ where the magnetization is continuous, showing that the transition is of second order. Comparison of the variational magnetization with the perturbative expression⁵ $\langle \sigma_3 \rangle_{\text{pert}} = 1 - 1/8\lambda^2$ is good for $\lambda > 1$.

If we now consider the variational method with the dual variables, defining the ground state of \tilde{H} , Eq. (3), in terms of an angle $\tilde{\theta}$ as in Eq. (4), the transition occurs at $\sin \tilde{\theta} = \lambda/2 = 1$. This means that the critical point is not uniquely predicted by the variational method. The second-order character of the transition is evident because of the continuity of the variational parameter θ (or $\tilde{\theta}$) through the critical point, but the order parameter expressed in dual variables is nonlocal and reads

$$\begin{aligned} \langle \tilde{\theta} | \sigma_3(n) | \tilde{\theta} \rangle &= \left\langle \tilde{\theta} \left| \sum_{\tilde{n} < n} \tilde{\sigma}_1(\tilde{n}) \right| \tilde{\theta} \right\rangle \\ &= \begin{cases} (\sin \tilde{\theta})^n & \text{for } \lambda < 2 \\ 1 & \text{for } \lambda > 2 \end{cases} \end{aligned}$$

which is not correct for finite values of λ above the critical point.

III. HAMILTONIAN Z(2) MODEL IN THREE SPATIAL DIMENSIONS

Defining σ_3 and σ_1 variables at each link of the cubic lattice of Fig. 3, the Hamiltonian

$$H = - \sum_{\text{links}} \sigma_1 - \lambda \sum_{\text{plaquettes}} \sigma_3 \sigma_3 \sigma_3 \sigma_3 \quad (6)$$

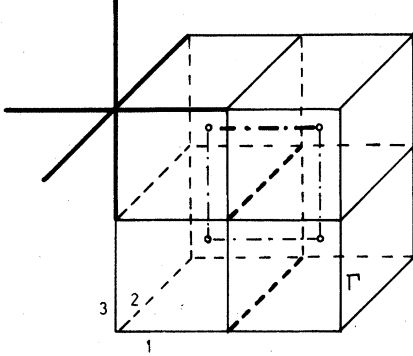


FIG. 3. $Z(2)$ three-dimensional lattice. Thick solid links are those affected by gauge transformation on a direct site. Open circles denote dual sites. Thick dashed lines show direct links involved in the definition of $\tilde{\sigma}_3$ on the dual link represented by a thick dashed-dotted line [see Eq. (7)]. Links on curve Γ in plane 1-3 are involved in the Wilson loop calculation [Eq. (9)]. Dual links starting from open circles along direction 2 are affected by Eq. (10).

is gauge invariant, i.e., $GHG^{-1}=H$ with $G = \prod_{i=1}^6 \sigma_i$ where the 6 links emerging from a particular site are included.

In the sector of gauge-invariant states the variables on the vertical links may be chosen $\sigma_3=1$ and their conjugate momenta σ_1 determined by the condition $G=1$. The model turns out to be self-dual since defining

$$\tilde{\sigma}_1 = \sigma_3 \sigma_3 \sigma_3 \sigma_3, \quad \tilde{\sigma}_3(1) = \prod_{\langle x_3 \rangle} \sigma_1(2), \quad \tilde{\sigma}_3(3) = 1, \quad (7)$$

as shown in Fig. 3, we may rewrite

$$\tilde{H} = H/\lambda = - \sum_i \tilde{\sigma}_i - \lambda^{-1} \sum_p \tilde{\sigma}_3 \tilde{\sigma}_3 \tilde{\sigma}_3 \tilde{\sigma}_3, \quad (8)$$

where the sum is now on the dual links and plaquettes. This result is gauge independent.

Since it has been proved⁹ that the ground state must be gauge invariant $G|0\rangle_\lambda = |0\rangle_\lambda$, we take as nonlocal order parameter the expectation value of the gauge-invariant operator given by the product of σ_3 along a closed loop Γ (Wilson loop)

$$C_\Gamma = \frac{\lambda \langle 0 | \sigma_3 \cdots \sigma_3 | 0 \rangle_\lambda}{\lambda \langle 0 | 0 \rangle_\lambda}. \quad (9)$$

If we use the dual variables we notice that \tilde{H} is invariant under $\tilde{G} = \prod_{p=1}^6 (\sigma_3 \sigma_3 \sigma_3 \sigma_3) = \prod_{i=1}^6 \tilde{\sigma}_i$, where the six links emerging from a dual site are normal to the six plaquettes p .

Taking a gauge-invariant ground state $\tilde{G}|\tilde{0}\rangle_\lambda = |\tilde{0}\rangle_\lambda$, we may calculate the order parameter as

$$\tilde{C}_\Gamma = \frac{\lambda \langle \tilde{0} | \sigma_3 \cdots \sigma_3 | \tilde{0} \rangle_\lambda}{\lambda \langle \tilde{0} | \tilde{0} \rangle_\lambda} = \frac{\lambda \langle \tilde{0} | \tilde{\sigma}_1 \cdots \tilde{\sigma}_1 | \tilde{0} \rangle_\lambda}{\lambda \langle \tilde{0} | \tilde{0} \rangle_\lambda}. \quad (10)$$

Then, as shown in Fig. 3, the order parameter

can be calculated alternatively either as the expectation value of the σ_3 's along a closed loop, Eq. (9), or as that of the product of the $\tilde{\sigma}_1$'s corresponding to the dual links perpendicular to all the direct plaquettes contained in the loop Γ , Eq. (10). We shall see that each treatment easily describes one of the phases.

Using the direct variables the gauge-invariant ground state will be obtained applying the operator G any number of times on a state $|\theta\rangle$ of the form of Eq. (4), but with product over all links instead of sites. For $\lambda \rightarrow \infty$ one expects $\theta \rightarrow 0$ so that the interference terms both in the numerator and denominator of Eq. (9) vanish and

$$C_\Gamma \xrightarrow{\lambda \rightarrow \infty} (\cos \theta)^P = \exp(P \ln \cos \theta), \quad (11)$$

where P is the perimeter of the loop Γ .

On the other hand the description with dual variables corresponds to applying the dual gauge operator \tilde{G} to $|\tilde{\theta}\rangle$. The variational angle $\tilde{\theta}$ is now expected to vanish for $\lambda \rightarrow 0$ so that in this limit the interference terms in Eq. (10) tend to disappear leaving as leading contribution

$$\tilde{C}_\Gamma \xrightarrow{\lambda \rightarrow 0} (\sin \tilde{\theta})^A = \exp(A \ln \sin \tilde{\theta}), \quad (12)$$

where A is the area enclosed by Γ .

We shall see in Sec. IV that the variational $|0\rangle_\lambda$ is not able to reproduce the area law for small λ whereas the dual variable state $|\tilde{0}\rangle_\lambda$ exhibits the perimeter behavior for large λ . This better description of the direct Wilson loop with the dual variational state can be understood by noticing that $|\tilde{0}\rangle_\lambda$, due to Eq. (7), contains overlap of direct spin states suitable to the study of correlation functions.

IV. ANALOGY OF THE VARIATIONAL $Z(2)$ WITH A CLASSICAL ISING MODEL

Starting from the non-gauge-invariant state

$$|\theta\rangle = \prod_{\text{links}} \begin{pmatrix} \cos \frac{1}{2} \theta \\ \sin \frac{1}{2} \theta \end{pmatrix}_i, \quad (13)$$

we obtain the gauge-invariant state $|0\rangle_\lambda = S|\theta\rangle$ with

$$S = \frac{1}{2} \prod_{\text{sites}} (1 + G_s) = \frac{1}{2} \prod_s \sum_{\mu_s} G_s^{(1-\mu_s)/2}, \quad (14)$$

where μ_s are variables defined on the sites and which may take the values ± 1 . Therefore the norm of the ground state may be written as

$$\begin{aligned} \lambda \langle 0 | 0 \rangle_\lambda &\propto \sum_{\{\mu_s\}} \prod_i (\sin \theta)^{(1-\mu_1 \mu_2)/2} \\ &= (\sin \theta)^{N/2} \sum_{\{\mu_s\}} \prod_i e^{\beta \mu_1 \mu_2}, \end{aligned} \quad (15)$$

where $e^{-2\beta} = \sin\theta$ and 1 and 2 denote the two sites joined by the link l . Therefore $\lambda\langle 0|0\rangle_\lambda$ is equivalent to the partition function of a classical three-dimensional Ising model with the correspondence

$$\lambda \rightarrow \infty, \beta \rightarrow \infty; \lambda \rightarrow 0, \beta \rightarrow 0. \quad (16)$$

In the evaluation of C_Γ [Eq. (9)] it is necessary that all the interference terms have the same value of μ along the loop, i.e., all the link spins must be nonflipped, giving

$$C_\Gamma = (\cos\theta)^P \frac{\sum_{\{\mu_s\}} \prod_l e^{\beta\mu_1\mu_2\delta_{\mu_1,\mu_2;i \in \Gamma}}}{\sum_{\{\mu_s\}} \prod_l e^{\beta\mu_1\mu_2}}. \quad (17)$$

It is clear that for $\beta \rightarrow \infty$ only the aligned configurations will survive and the perimeter law equation (11) emerges.

Regarding the calculation of $E(\theta)$, the plaquette terms will be analogous to Eq. (17) whereas each link term will include

$$\frac{\lambda\langle 0|(\sigma_l)_l|0\rangle_\lambda}{\lambda\langle 0|0\rangle_\lambda} = \frac{\sum_{\{\mu_s\}} (\sin\theta)^{(\mu_1\mu_2)l} \prod_{l'} e^{\beta(\mu_1\mu_2)l'}}{\sum_{\{\mu_s\}} \prod_{l'} e^{\beta(\mu_1\mu_2)l'}}. \quad (18)$$

With the number of the links and plaquettes related by $N_l/N_p = 2, 1$ for $D = 2, 3$ dimensions, the energy per link will be

$$-\frac{E(\theta)}{N_l} = \langle e^{-2\beta(\mu_1\mu_2)l} \rangle + \frac{D-1}{2} \lambda (\cos\theta)^4 \langle \delta_{\mu_1,\mu_2;i \in p} \rangle, \quad (19)$$

where $\langle \rangle$ indicates the statistical average.

Using the dual variables we have again an equivalent classical system of spins $\tilde{\mu}$ with the correspondence

$$\lambda \rightarrow 0, \tilde{\beta} \rightarrow \infty; \lambda \rightarrow \infty, \tilde{\beta} \rightarrow 0, \quad (20)$$

and the Wilson loop, in the form of Eq. (10), is given by

$$\tilde{C}_\Gamma = (\sin\tilde{\theta})^A \left\langle \prod_{\tilde{l} \in A} e^{2\tilde{\beta}(1-\tilde{\mu}_1\tilde{\mu}_2)} \right\rangle, \quad (21)$$

where the links \tilde{l} , which are inside the loop Γ , join the dual classical spins $\tilde{\mu}_1$ and $\tilde{\mu}_2$. For $\lambda \rightarrow 0$ all the dual spins tend to be aligned, the statistical average of Eq. (21) tends to 1, and the Wilson loop shows the area behavior. Since for infinite lattices self-duality is exact, the energy $\tilde{E}(\tilde{\theta})$ has the same form of Eq. (19) with the replacement $\lambda \rightarrow 1/\lambda$.

To compute the above expressions we turn now to approximate methods¹⁶ comparing the three- and two-dimensional cases.

(i) *Low-temperature expansions.* Including up to four spin-flip configurations and letting $x = \sin\theta$ we obtain

$$\langle e^{2\beta(1-\mu_1\mu_2)l} \rangle = \begin{cases} 1 + 2x^4 - 2x^6 + 10x^8 - 24x^{10} + 84x^{12} - 246x^{14}, & D=3 \\ 1 + 2x^2 + 4x^4 + 12x^6 + 24x^8, & D=2 \end{cases} \quad (22)$$

and similarly with up to three spin flips we obtain

$$\langle \delta_{\mu_1\mu_2;i \in p} \rangle = \begin{cases} 1 - 4x^6 - 20x^{10} + 30x^{12} - 140x^{14}, & D=3 \\ 1 - 4x^4 - 12x^6 - 30x^8, & D=2 \end{cases} \quad (23)$$

to have the same powers in the link and plaquette terms.

With the above expansions Eqs. (22) and (23) we may calculate $f(x) = -E(\theta)/N_l$ [Eq. (19)]. It is clear that $f(x)$ will have a maximum for a small value of x , for λ not too small, the region where the expansions in Eqs. (22) and (23) are valid.

Regarding the Wilson loop we have

$$C_\Gamma \xrightarrow{\beta \rightarrow \infty} \begin{cases} (\cos\theta)^P [1 - P(x^6 + 5x^{10})], & D=3 \\ (\cos\theta)^P [1 - P(x^4 + 3x^6)], & D=2 \end{cases} \quad (24)$$

confirming the perimeter law for large λ .

(ii) *High-temperature expansions.* Considering up to eight-link closed contributions the expansions in powers of $y = \tanh\beta$ are

$$\langle e^{-2\beta(\mu_1\mu_2)l} \rangle = \begin{cases} 1 - 8y^4 - 88y^6, & D=3, \\ 1 - 4y^4 - 12y^6 - 36y^8, & D=2. \end{cases} \quad (25)$$

and similarly

$$\langle \delta_{\mu_1 \mu_2; i \in P} \rangle = \begin{cases} \frac{1}{8}(1+y)^4(1+12y^3-5y^4+108y^5), & D=3 \\ \frac{1}{8}(1+y)^4(1+4y^3-5y^4+12y^5-6y^6+16y^7), & D=2. \end{cases} \quad (26)$$

With $\sin \theta = (1 - \tanh \beta)/(1 + \tanh \beta)$, Eq. (19) takes the form

$$f(y) = \begin{cases} 1 + 2\lambda y^2 - 8y^4 + 24\lambda y^5 - (88 + 10\lambda)y^6 + 216\lambda y^7, & D=3 \\ 1 + \lambda y^2 - 4y^4 + 4\lambda y^5 - (12 + 5\lambda)y^6 + 12\lambda y^7 - (36 + 6\lambda)y^8 + 16\lambda y^9, & D=2. \end{cases} \quad (27)$$

From Eq. (27) one sees that for λ not too large, $f(y)$ has a maximum for small y the region where the expansion is valid. Therefore, we may suspect that increasing λ the absolute maximum jumps from the high-temperature maximum (small $\cos \theta$) to the low-temperature one (large $\cos \theta$). It is noteworthy, comparing Eqs. (22), (23), and (27), that if for $D=2$ we double the value of λ the low-temperature maximum remains almost at the same position as for $D=3$ whereas the high temperature maximum is more on the right in a $\cos \theta$ plot. Then it is conceivable that in the two-dimensional case the high-temperature maximum disappears when the low-temperature one appears with a continuous change in agreement with the second-order transition of its dual Ising model.

We notice that the direct variable variational model fails to predict the area behavior of the Wilson loop for small values of λ . In fact for large square loops we obtain

$$C_\Gamma \xrightarrow{\beta \rightarrow 0} 2y^{P/2} [1 + 4y^2 + 2(D-1)y^3P], \quad (28)$$

i.e., again a perimeter law. One must remark that the phase transition is still described by the discontinuities of the derivatives of the minimum of $E(\theta)$ with respect to λ .

(iii) *Expansions with dual variables for $D=3$.* For $\tilde{\beta} \rightarrow \infty$ the Wilson loop equation (21) in the two-spin-flip limit takes the form

$$\tilde{C}_\Gamma \underset{\tilde{\beta} \rightarrow \infty}{\sim} (\sin \tilde{\theta})^A [1 + 2A \sin^4 \tilde{\theta} (1 + \sin^2 \tilde{\theta})], \quad (29)$$

whereas for $\tilde{\beta} \rightarrow 0$ since

$$\sum_{\{\mu\}} \prod_{i \in A} e^{-2\tilde{\beta}(\tilde{\mu}_1 \tilde{\mu}_2) \tilde{i}} \prod_{i'} e^{\tilde{\beta}(\tilde{\mu}_1 \tilde{\mu}_2) \tilde{i}'} = (\cosh \tilde{\beta})^{N_A} \sum_{\{\mu\}} \prod_{i \in A} (1 - \tilde{\mu}_1 \tilde{\mu}_2 \tanh \tilde{\beta}) \prod_{i' \neq i} (1 + \tilde{\mu}_1 \tilde{\mu}_2 \tanh \tilde{\beta}),$$

the six-link closed path approximation gives

$$\tilde{C}_\Gamma \underset{\tilde{\beta} \rightarrow 0}{\sim} 1 - 2P \tanh^4 \tilde{\beta} (1 + 16 \tanh^2 \tilde{\beta}). \quad (30)$$

Therefore, as anticipated in Sec. III, the use of the dual variational state $|\tilde{0}\rangle_\lambda$ allows one to describe the passage of the direct Wilson loop from an area law for small λ to a perimeter behavior for large λ . This is due to the fact that $|\tilde{0}\rangle_\lambda$ overlaps the direct individual spin states. It is clear that, symmetrically, the analysis of the phase transition is correctly described by the direct state $|0\rangle_\lambda$ examining the dual Wilson loop $\langle \tilde{\sigma}_3 \cdots \tilde{\sigma}_3 \rangle$. One has to note that, though the adopted order parameter may be partially in conflict with the variational treatment as indicated also in Sec. II, both $|0\rangle_\lambda$ and $|\tilde{0}\rangle_\lambda$ are able to describe the phase transition looking at the derivatives of the minimum of the energy with respect to λ . For the former, Eq. (19) is in order with $D=3$ and for the latter, one simply replaces $\lambda \rightarrow 1/\lambda$. The result regarding the nature of the phase transition

will be the same.

(iv) *Numerical results.* Because of the equivalence of our variational treatment with a classical Ising model one expects the above low- and high-temperature expansions to be valid at each side of its critical point, i.e., $\cos^2 \theta \approx 0.83$ and $\cos^2 \theta \approx 0.58$ for $D=2$ and $D=3$, respectively.

Looking at Eqs. (22), (23), and (27) one sees that higher powers of x have been included in the low-temperature expansion for $D=3$ in comparison to the high-temperature series. The reason is that for this case the value of x near the Ising critical point is larger than the corresponding value of y , at variance with the $D=2$ case where both values are similar. This demonstrates that, as shown in Figs. 4 and 5, the convergence of all series is fast except for the low-temperature expansion for $D=3$ between $x \approx 0.5$ and the Ising critical point. So, whereas for $D=2$ Fig. 4 indicates that no minimum of f appears, for $D=3$ Fig. 5 shows a minimum between the regions of convergence of the high- and low-temperature ex-

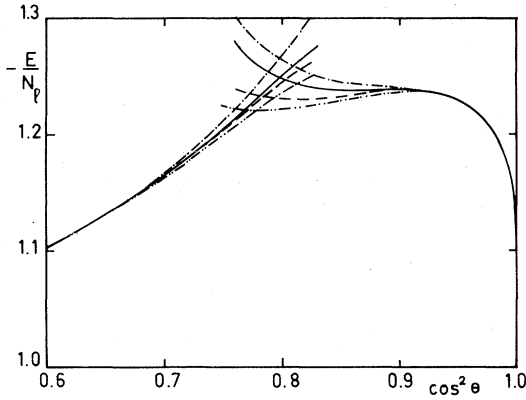


FIG. 4. Convergence of low-temperature (right) and high-temperature (left) expansion for $D=2$ and $\lambda=2.2$. Complete series Eqs. (22), (23), and (27) are represented by solid lines, dropping $24x^8$ and $16\lambda y^9$ by dashed lines, omitting $-30x^8$ and $-(36+6\lambda)y^8$ by dashed-dotted lines, and neglecting $12x^6$ and $12\lambda y^7$ by dashed-double-dotted lines.

pansions for the chosen value of λ . To improve the convergence of the latter we have used diagonal Padé approximants obtaining in this way smooth matching for all cases close to the Ising critical point.

We may similarly analyze the curve f for all values of the variational parameter θ and the coupling λ as represented in Figs. 6 and 7 for $D=2$ and 3, respectively. These curves are calculated taking the average of the expansions with or without the last term except for the low-temperature $D=3$ case where the (7,7) Padé approximant, almost coincident with the (6,6) one, is considered. The important feature of Figs. 6 and 7, stable against the addition of high-power corrections, is that for a range of λ there is a minimum between two maxima for $D=3$ which does

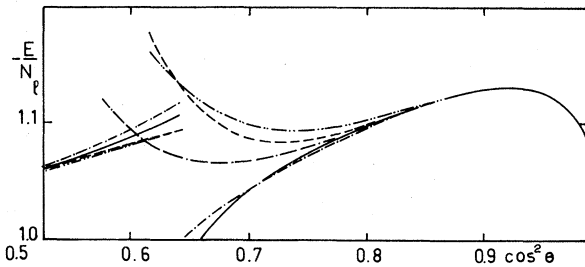


FIG. 5. Convergence of low-temperature (right) and high-temperature (left) expansions for $D=3$ and $\lambda=1$. Complete series Eqs. (22), (23), and (27) are represented by solid lines, dropping x^{14} and y^7 terms by dashed lines, omitting x^{12} and y^6 terms by dashed-dotted lines, and neglecting x^{10} and y^5 terms by dashed-double-dotted line. Dotted-double-dashed line indicates the Padé (7,7) approximant for the low-temperature expansion.

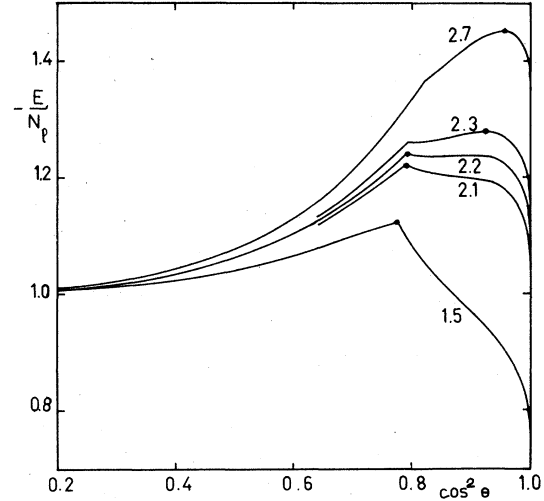


FIG. 6. $D=2$ variational energy. $f = -E/N_f$ is calculated using the average of solid and dashed curves of Fig. 4. The numbers on the curves denote the values of λ and the full dots the maxima of f . From $\lambda=2.2$ to $\lambda=2.3$ there is a plateau suggesting a continuous shift of f_{\max} .

not appear for $D=2$.

For $D=2$ it is seen that by increasing λ the maximum f_{\max} of $f(\cos^2 \theta)$ moves quickly from $\cos \theta = 0$ to a value close to that of the critical Ising model for low values of λ . The value of f_{\max} remains at the point of intersection of both expansions up to $\lambda \approx 2.22$ when the maximum starts moving continuously in the low-temperature region. This is in agreement with a second-order transition since,

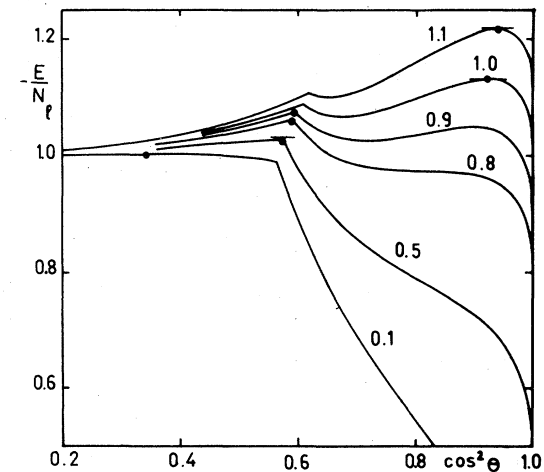


FIG. 7. $D=3$ variational energy. f is calculated using the average of solid and dashed curves (left) and Padé approximants (right) of Fig. 5. The small horizontal segments in correspondence to the maxima indicate the perturbative values according to Eq. (31). From $\lambda=0.9$ to $\lambda=1$, f_{\max} jumps discontinuously to the right.

as shown in Fig. 8, the plot of $f_{\max}(\lambda)$ appears to be the union at the critical point of two curves presenting, within the precision of the series in that region, a discontinuity in the second derivative. The critical value of λ should be compared with the result $\lambda_c \approx 3.28$ obtained by renormalization-group analysis.^{11,13} On the other hand the variational approach gives for the dual two-dimensional Ising model with transverse field a critical point $\lambda_c = 4$ instead of $\lambda_c \approx 3$ which results again from the renormalization group.¹⁵

For $D=3$ there is a clear qualitative difference. For low values of λ there is a single maximum of f in the high-temperature region which reaches the classical Ising critical point, but for increasing λ a second maximum appears in the low-temperature zone. Beyond $\lambda \approx 0.94$ the latter becomes the absolute maximum and the corresponding variational parameter $\cos^2 \theta$ jumps discontinuously from ~ 0.6 to ~ 0.9 . This characterizes a first-order transition in agreement with the result of Ref. 12. Obviously the same conclusion can be drawn from Fig. 9 where it is seen that the first derivative of $f_{\max}(\lambda)$ is discontinuous. Since for $D=3$ the model is self-dual, the analysis using dual variables gives the same result with a critical value of λ again ~ 1 .

Regarding the Wilson loop for $D=3$, Eq. (24) gives a clear perimeter law for $\lambda > \lambda_c$ when the value of x corresponding to f_{\max} is inserted. For $\lambda < \lambda_c$ the high-temperature expression Eq. (28) does not reproduce the expected area law. On the other hand, the dual variable calculation for $\lambda < \lambda_c$ [Eq. (29)] gives a neat area behavior, whereas

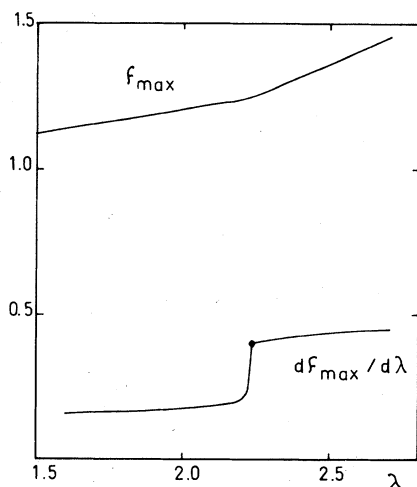


FIG. 8. $D=2$ maxima of f and first derivative with respect to the coupling constant. The full dot denotes the point where a discontinuity in the second derivative is apparent. Precise determination is obscured by uncertainty of f_{\max} for $2.2 < \lambda < 2.3$.

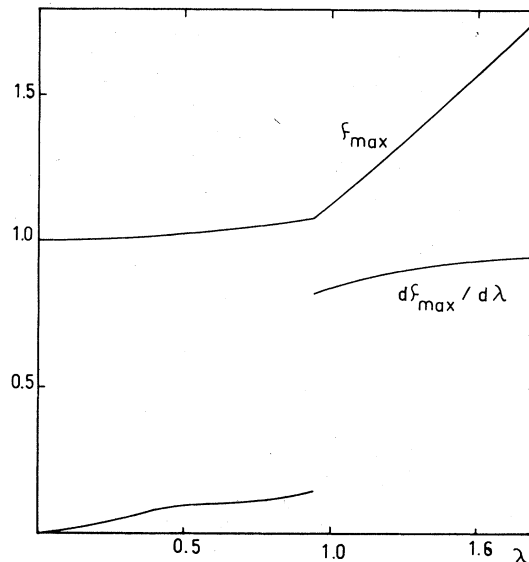


FIG. 9. $D=3$ maxima of f and first derivative with respect to the coupling constant. The discontinuity in $df_{\max}/d\lambda$ shows the first-order character of the transition.

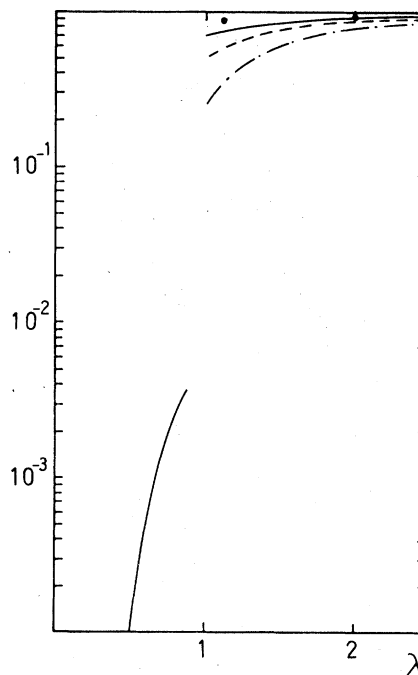


FIG. 10. $D=3$ Wilson loop. The direct variable expansion C_Γ , Eq. (24), is shown on the right of $\lambda = 0.94$ and the dual variable calculation \tilde{C}_Γ on the left. The solid, dashed, and dashed-dotted curves correspond to values of $P=8, 16, 32$ ($A=4, 16, 64$), respectively. The curves for $A=16$ and 64 , not shown on the left, are in excellent agreement with an area law. The full dots represent Eq. (30) for $P=8$.

for $\lambda > \lambda_c$ the values predicted by Eq. (30) are in reasonable agreement with those obtained from the direct variable expression Eq. (24). These features are shown in Fig. 10, indicating that the dual variational states give a better description of the direct Wilson loop.

Finally, we wish to remark that the agreement of the energy obtained with the variational method and that calculated with perturbative expansions is excellent. The former corresponds to the maxima of $f(x)$ shown in Fig. 7 and the latter is⁵

$$\frac{E_{\text{pert}}}{N_t} = \begin{cases} -1 - \frac{1}{8}\lambda^2 - \frac{3}{512}\lambda^4, & \lambda < 1 \\ -\lambda \left(1 + \frac{1}{8} \frac{1}{\lambda^2} + \frac{3}{512} \frac{1}{\lambda^4} \right), & \lambda > 1. \end{cases} \quad (31)$$

Only for $0.8 < \lambda < 0.94$ E_{pert} , which converges quickly, is slightly higher than f_{max} giving further support to the existence of a minimum for f .

V. CONCLUSIONS

We briefly summarize the achievements of our variational method in the analysis of the Hamiltonian $Z(2)$ gauge model.

(i) From the requirement of gauge invariance of the ground state we show the equivalence with a classical Ising model.

(ii) Low- and high-temperature expansions allow one to evaluate the variational energy. For three spatial dimensions the variational parameter shows a discontinuous change for a critical value of the coupling constant giving evidence for a first-order transition in agreement with Ref. 12. For two spatial dimensions the variational parameter changes continuously, but it is apparent that the second derivative of the variational energy with respect to the coupling constant is discontinuous for a critical point. This is in agreement with the second-order transition which is known to appear in its dual model, the Ising model

with transverse field.

(iii) The phase transition for $D=3$ is characterized by the change of the nonlocal order parameter, the Wilson loop, from an area behavior (electric confining phase) to a perimeter one (electric free phase). This follows from the use of the dual variational ground state because of the overlapping of direct spin states contained in it.

(iv) For $D=3$ the variational treatment with direct variables predicts a critical value of the coupling constant $\lambda_c \approx 0.94$ compared to the symmetry point $\lambda=1$ and, for $D=2$, $\lambda_c \approx 2.22$ to be compared with the value 3.28 resulting from renormalization-group analysis.^{11,13}

(v) The variational energy turns out to be in good agreement with the perturbative expansions.

Having shown that the variational method is able to demonstrate the nature of the phase transition of the Hamiltonian $Z(2)$ model with a quantitative accuracy for the three-dimensional case, we hope to generalize it to $Z(N)$ to corroborate the three-phase diagram suggested by several authors¹⁷ for sufficiently large N . It would also be interesting to investigate why the renormalization-group methods fail to predict the first-order transition in the three-dimensional Hamiltonian $Z(2)$ model.

Note added. After the completion of the present work we received a report by Cardy and Hamber¹⁸ where similar conclusions regarding the first-order transition of the three-dimensional case are obtained using overlapping variational ground states, and another by Drouffe⁹ where the same result is reached through strong-coupling expansions.

ACKNOWLEDGMENTS

We thank our colleagues of the Particle Group of the La Plata University for very useful discussions.

¹G. 't Hooft, Nucl. Phys. **B138**, 1 (1978); **B153**, 141 (1979).

²F. Wegner, J. Math. Phys. **12**, 2259 (1971).

³S. Edwards and P. Anderson, J. Phys. F **5**, 965 (1975).

⁴B. Halperin and D. Nelson, Phys. Rev. Lett. **42**, 121 (1978); Phys. Rev. B **19**, 2457 (1979).

⁵E. Fradkin and L. Susskind, Phys. Rev. D **17**, 2637 (1978).

⁶M. Weinstein, in *Proceedings of the Banff Summer Institute on Particles and Fields, Banff, 1977*, edited by D. H. Boal and A. N. Kamal (Plenum, New York, 1978).

⁷S. Tyablikov, *Methods in the Quantum Theory of Magnetism* (Plenum, New York, 1967).

⁸R. Balian, J. Drouffe, and C. Itzykson, Phys. Rev. D **10**, 3376 (1974); **11**, 2098 (1975); **11**, 2104 (1975).

⁹S. Elitzur, Phys. Rev. D **12**, 3978 (1975).

¹⁰K. Wilson, Phys. Rev. D **10**, 2445 (1974).

¹¹E. Fradkin and S. Raby, Phys. Rev. D **20**, 2566 (1979).

¹²M. Creutz, L. Jacobs, and C. Rebbi, Phys. Rev. Lett. **42**, 1390 (1979); Phys. Rev. D **20**, 1915 (1979).

¹³D. Horn and S. Yankielowicz, Nucl. Phys. **B161**, 533 (1979).

¹⁴A. Migdal, Zh. Eksp. Teor. Fiz. **69**, 810 (1975); **69**, 1457 (1975) [Sov. Phys.—JETP **42**, 413 (1975); **42**, 743 (1975)]; L. Kadanoff, Ann. Phys. (N. Y.) **100**, 359 (1976).

- ¹⁵D. Mattis and J. Gallardo, Polytechnic Institute of New York report, 1979 (unpublished); K. Penson, R. Jullien, and P. Pfeuty, Phys. Rev. B 19, 4653 (1979).
- ¹⁶H. Stanley, *Introduction to Phase Transitions and Critical Phenomena* (Clarendon, Oxford, 1971).
- ¹⁷D. Horn, M. Weinstein, and S. Yankielowicz, Phys. Rev. D 19, 3715 (1979); S. Elitzur, R. Pearson, and J. Shigemitsu, *ibid.* 19, 3698 (1979); A. Ukawa, P. Windey, and A. Guth, *ibid.* 21, 1013 (1980); J. Cardy, J. Phys. A. 13, 1507 (1980); D. Boyanovsky, Nuovo Cimento 54A, 451 (1979); M. Einhorn, R. Savit, and E. Rabinovici, Michigan Report No. UM HE 79-25, 1979 (unpublished).
- ¹⁸J. Cardy and H. Hamber, Santa Barbara Report No. UCSB TH-33, 1979 (unpublished).
- ¹⁹J. Drouffe, Saclay Report No. DPh-T/79/169, 1979 (unpublished).